RSC Advances

PAPER

View Article Online
View Journal | View Issue

Cite this: *RSC Adv.*, 2016, **6**, 114644

Reduced use of glucose by normoxic cow's mammary gland under acute inflammation: an example of homeostatic aerobic glycolysis

Nissim Silanikove,*[a] Fira Shapiro,[a] Uzi Merin,[b] Yaniv Lavon,[c] Shlomo E. Blum[d] and Gabriel Leitner[d]

The concentrations of glucose and glucose-derived carbons in milk reflect their concentrations in the mammary epithelial cell cytosol. We hypothesized that the sharp reduction in milk secretion observed during acute inflammation in the mammary gland is associated with conversion of the gland's metabolism to aerobic glycolysis and reduced extraction of glucose from the blood, in support to the innate immune system. Acute inflammation was induced by challenging one mammary gland in 5 cows with a single dose of 10 μg bacterial lipopolysaccharide. The glandular response was followed up to 96 h post-challenge. The challenge induced increases in polymorphonuclear leukocytes, milk malondialdehyde concentration and casein degradation. The response peaked at 24 h post-challenge and the inflammation began to decrease after 48 h, but at 96 h post-treatment, values had not yet returned to pre-treatment levels. Milk secretion, and milk lactose, glucose and citrate concentrations decreased sharply, reaching minimal levels at 24 h post-treatment. The correlations between these parameters and inflammation parameters were negative and statistically significant. The reduction of ~50% in milk yield and lactose concentration in the treated gland indicated that extraction of glucose from the blood was reduced from a rate of ~740 g d^{-1} to 190 g d^{-1} (*i.e.*, by 550 g d^{-1}) at the peak of response. The concentrations of glucose-6-phosphate, malate, oxaloacetate, lactate and pyruvate and the activities of the enzymes glucose-6-phosphate dehydrogenase, malate dehydrogenase and lactate dehydrogenase increased and, in general, were positively and significantly correlated to inflammation parameters. It was concluded that inflammation shifts the passage of glucose-derived carbons to the pentose phosphate pathway and shifts cell metabolism to glycolysis at the expense of mitochondrial activity.

Received 14th September 2016
Accepted 1st December 2016

DOI: 10.1039/c6ra22934d

www.rsc.org/advances

Introduction

Eukaryotic cells obtain energy through the oxygen-dependent pathway of oxidative phosphorylation (OxPhos) and the oxygen-independent pathway of glycolysis. Since OxPhos is far more efficient at generating ATP than glycolysis, the presence of oxygen results in activation of the former and inhibition of the latter (termed Pasteur effect).[1] Otto Warburg showed that tumor cells produce large amounts of lactate (La), even in the presence of oxygen,[2] a condition that is commonly known as the Warburg effect, or aerobic glycolysis (AG). AG is commonly regarded as the hallmark of cancer and tumor malignancy.[1]

Studies have shown that the concentration of metabolites produced and secreted by mammary epithelial cells (MECs) in humans,[3,4] rats,[5] cows[6] and ruminants[7,8] is closely associated with MEC metabolic state. Those studies were then substantiated by more recent ones showing that the concentration of glucose (G) and G-derived carbons in cow's milk reflects metabolic function in MECs.[9–11]

In particular, evidence has suggested that modifications in milk concentration of La, malate (Ma) and citrate (Cit) under acute[12] and chronic immune stress,[10] and under pro-involution conditions (milk stasis),[13] reflect conversion of the mammary gland metabolism to glycolysis at the expense of OxPhos. In modern dairy cows, ~80% of the G turnover is diverted to the mammary gland,[14] supporting the high metabolic demand (4- to 5-fold maintenance requirements) for milk production.[15] Ongoing inflammatory and immune responses are associated with dramatic shifts in tissue metabolism and G requirements.[16] The increased demand for G results from intense proliferation and recruitment of inflammatory cell types, particularly myeloid cells, such as neutrophils (polymorphonuclear leukocytes

[a]*Department of Ruminant Science, Animal Science, The Volcani Center, P.O. Box 6, Bet Dagan 50250, Israel. E-mail: nissim.silanikove@mail.huji.ac.il*

[b]*Food Quality and Safety, Postharvest and Food Sciences, The Volcani Center, P.O. Box 6, Bet Dagan 50250, Israel*

[c]*Israel Cattle Breeders Association, Caesarea, Israel*

[d]*National Mastitis Reference Center, Kimron Veterinary Institute, P.O. Box 12, Bet Dagan 50250, Israel*

[PMNs]) and monocytes.[16] Cells of the myeloid lineage derive their energy almost exclusively from glycolysis,[16] which amplifies their need for G under acute inflammation.[17] It has been suggested that the conversion of MEC metabolism to increased AG at the expense of OxPhos is the main mechanism translating the milk-borne negative-feedback signals arising from, for example, acute immune stress and milk stasis into reduced MEC activity and milk secretion. This process then enhances G availability to support the immune system.[10–13] Nevertheless, those previous studies lack information on key metabolites shifting MEC to AG, which is reflected by changes in G, G-derived carbons and key enzyme activities in milk.

The present study tested the outcome of bacterial lipopolysaccharide (LPS) challenge of the mammary gland. The hypothesis was to test whether under the acute inflammatory stress the metabolic activities of MECs shifts to predominantly AG and are associated with reduced G extraction from the blood, reduced lactose secretion and milk yield. Such changes should be reflected by the concentrations of G, G-6-phosphate (G6P), pyruvate (Pyr), La, oxaloacetate (OA) and Ma and by the activities of glucose-6-phosphate dehydrogenase (G6PD), lactate dehydrogenase (LDH) and malate dehydrogenase (MDH) in milk. We hypothesize that these responses are induced by the acute inflammatory reaction and therefore should be closely related to measures of inflammation (leukocyte counts) and the oxidative stress marker malondialdehyde (MDA).

Materials and methods

Ethics

All protocols were approved by the Institutional Animal Care Committee of the Agricultural Research Organization, The Volcani Center, the legitimate body for such authorizations in Israel (No. b8974_18_015).

Experimental design

Five Israeli Holstein cows in their first to third lactation and 100–500 d in milk (days after parturition), yielding 28.1 ± 3.1 L milk d^{-1} and free of bacterial infection were chosen for LPS intramammary challenge (IMC). One week before the start of the experiment, the 5 cows were moved to a separate yard that provided 10 m^2 of shaded slatted floor. Before and during the experiment, the cows were fed a typical Israeli total mixed ration (17% protein) containing 65% concentrate and 35% forage, which were offered *ad libitum* in mangers. Water was available at all times. The experiment was carried out in November under a natural lighting regime, with typical noon temperatures of 24 °C and night temperatures of 12 °C, which are considered favorable for cow welfare.[18] Cows were milked thrice daily (05:30, 12:30, and 21:30 h) and individual milk yield was recorded automatically (AfiFarm Herd Management Software, Afimilk, Afikim, Israel). Milk gross composition: fat, protein and lactose content were analyzed at the Israel Cattle Breeders Association Central Laboratory (Caesarea, Israel) using the Milkoscan FT+ and somatic cell count (SCC) by the Fossomatic FC (Foss Electric, Hilleröd, Denmark).

Before challenge, milk yield, composition, bacteriology, SCC and leukocyte distribution were evaluated before treatments at −2 d and d 0 (day of treatment), separately for each gland. Experimental procedures were carried out during the milking except for the first sampling, which was performed 3 h after challenge. Intramammary inoculation was performed aseptically after the morning milking. Teats were thoroughly cleaned, dried, disinfected with iodine and wiped with antiseptic cloth (MediWipes, Al-Baad, Massuot Itzhak, Israel). One gland in each cow was infused with 10 μg LPS (*Escherichia coli* O55B5; Sigma Chemical Co., St. Louis, MO) dissolved in 10 mL sterile non-pyrogenic saline (Teva Pharmaceutical Industries Ltd., Petach Tikva, Israel), whereas the other 3 glands served as treatment controls. Development of clinical symptoms was recorded during the first 24 h, including rectal temperature measurements every 4 h. At 0 h, and +3, 6, 12, 24, 48, 72 and 96 h, the challenged glands and the 3 control glands of each cow were milked separately into individual containers and milk samples were taken after recording milk yield.

Analytical procedures

One subset of samples was sent to a central laboratory for the determination of fat, protein and casein.[19] Somatic cell distribution was assessed by flow cytometry (FACS Calibur, Becton-Dickinson, San Jose, CA) as described previously.[20] Additional subsets of milk samples (~50 mL) were defatted under cold conditions[21] and analyzed for lactose, La, Ma, OA, Cit, G and G6P by enzymatic reactions coupled to formation of a chromophore.[10,12,22] The concentrations of these metabolites were determined in whole milk samples by classical enzymatic reactions that use dehydrogenases (NAD^+/P^+-dependent oxidoreductases) coupled to conversion of NAD^+/P^+ to NADH/NADPH + H^+. The last stage in these determinations was linked to the formation of the fluorochromophore as follows:

$$\mathrm{NADH} + \mathrm{H}^+ \xrightarrow{\text{resazurin+diaphorase}} \mathrm{NAD}^+ + \text{resorufin}. \quad (1)$$

Using simple modifications, applying established reaction conditions, it is possible to determine the activity of key NAD^+/P^+-dependent oxidoreductases that are associated with G6P, Ma and Pyr reduction. We used this principle to determine the activity of G6PD, MDH and LDH in milk samples. The final activity of diaphorase and the concentration of resazurin used for these enzyme-activity determinations were the same as used for the metabolite determinations. The reaction conditions for G6PD activity in milk were according to the assay procedure of Gumaa *et al.*[23] The concentration of NADPH at the linear stages of the reaction (2 and 7 min after the start of the reaction in the present case) was calculated from a standard containing variable levels (between 10 and 1000 μM) of NADPH, which was converted to $NADP^+$ by diaphorase and coupled to the conversion of resazurin to the highly fluorimetric resorufin (r^2 = 0.988). The differences in NADPH concentration were divided by time and were converted to activity, where 1 U of G6PD activity oxidizes 1.0 μmol L^{-1} of D-G6P to 6-phospho-D-gluconate per minute in the presence of $NADP^+$ at pH 7.4, 25 °C. The

basic reaction conditions for MDH activity in milk were as described by Rokosh *et al.*[24] The differences in NADH concentration (between 10 and 1000 μM) at the linear stage of the reaction were divided by time and were converted to activity where 1 U of MDH will convert 1.0 μmol L^{-1} OA and NADH to L-malate and NAD^+ per minute at pH 7.5 at 25 °C. The reaction conditions for LDH activity were as described by Larsen.[25] One international unit of LDH activity was defined as the amount of enzyme that catalyzes the conversion of Pyr into La to generate 1.0 μmol L^{-1} of NAD^+ per minute at 37 °C.

The concentration of MDA was determined in the milk samples by the fluorimetric thiobarbituric acid reactive substance assay of Feldman.[26]

Statistical analysis

The data sets in this study were analyzed using repeated-measures analysis (PROC MIXED) modeling which correlated residuals within cow (version 9.2, SAS Institute, Cary, NC). The analysis focused on the effects of time during the experiment on the level of a specific variable. Five dairy cows were tested for levels of 47 different variables during the time course of the experiment. The model used was: specific variable = time, where there are 8 time points from 0 to 96 h post-LPS infusion. Correlation models of all tested variables were performed using SAS Proc Corr.[27] Data are presented as means and SEM.

Results

Effect of intramammary challenge with LPS on inflammatory indices and oxidative-stress markers

Use of the same type and dose of LPS used herein to induce mammary gland inflammation showed significant initial responses of elevated rectal temperature, heart rate, respiration rate and plasma cortisol concentration within 3–4 h; these responses peaked within 4–6 h and returned to pre-IMC levels at about 10 h post-treatment.[28] The LPS-IMC-induced an acute inflammatory response in the treated gland was reflected by elevation of SCC and activity of the lysosomal enzyme β-*N*-acetyl-D-glucosaminidase in milk.[12,28] LPS-IMC-induced elevation of SCC consisted mainly of leukocytes, mostly PMNs ($CD18^+$ marked cells; Fig. 1). However, in contrast to the brief transient response in rectal temperature, respiration rate, heart rate and plasma cortisol levels, SCC reached peak levels at 24 to 48 h after treatment and started to decline thereafter, but did not return to pre-treatment levels at 96 h post-treatment. These results are consistent with previous reports showing that it takes about a week for SCC to return to pre-treatment levels after LPS-IMC.[12]

LPS-IMC induced an increase in the content of MDA in milk and a reduction in percent casein out of total proteins (Fig. 2), indicating casein degradation.[29] The kinetics of MDA and % casein changes over time paralleled the kinetics of log SCC changes and was reflected by a significant interrelationship between log SCC and MDA concentration (Table 1).

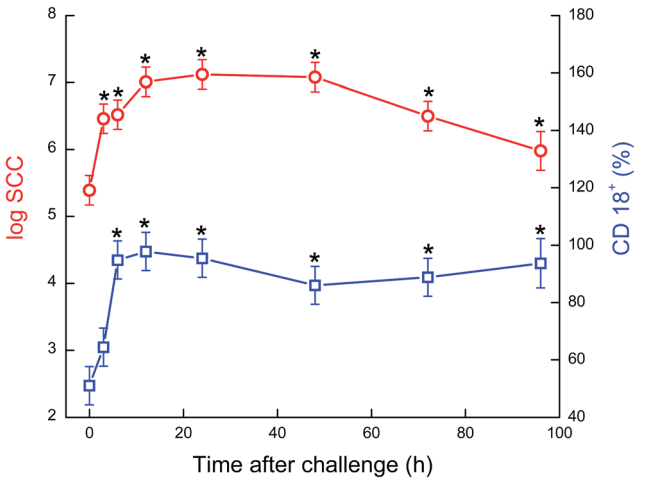

Fig. 1 Effect of challenging a single mammary gland of a cow's udder (5 cows) with lipopolysaccharide on the ontogenesis of log somatic cell count (log SCC) (○) and the proportion of leukocytes ($CD18^+$) (□) for up to 96 h. * indicates significant difference at $P < 0.01$.

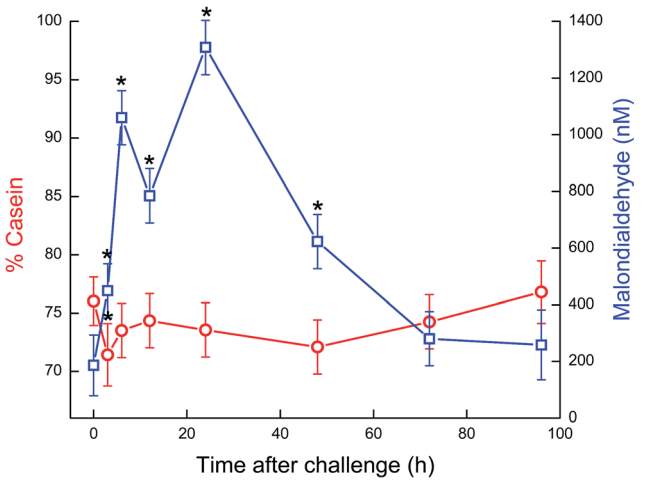

Fig. 2 Effect of challenging a single mammary gland of a cow's udder (5 cows) with lipopolysaccharide on the ontogenesis of % casein (○) and malondialdehyde (□) for up to 96 h. * indicates a significant difference at $P < 0.01$.

Effect of LPS-IMC on milk yield and lactose concentration

Average milk yield of all cows was 28.1 ± 3.1 L d^{-1} before the start of the experiment (Fig. 3). LPS-IMC induced a significant transient decrease in milk yield to 21.9 L ± 2.5 L d^{-1} at 24 h post-treatment on the whole gland level. Based on previous studies, it is assumed that the vast majority of the reduction occurred in the treated gland.[12,28] This phenomenon is consistent with previous experiments in which the same dose and type of LPS were applied, resulting in a maximal decrease of ~50% in milk yield, which was recorded 24 h post-treatment and ~20% decrease at 48 h post-treatment.[12,28] At 96 h post-treatment, the reduction in milk yield resumed to pre-treatment levels (Fig. 3). In previous studies[12,28] and the current one, the reductions in milk yield were closely associated with a marked reduction of

Table 1 Pearson correlation matrix among the measures applied to follow the response to challenge of a single mammary gland with lipopolysaccharide[a]

	1	2	3	4	5	6	7	8	9	10	11	12	13	14	15	16	17	18	19	20	21
	SCC	Casein	Lactose	CD18$^+$	PMN	La	Ma	Cit	OA	Pyr	G6P	G	G6PD	LDH	MDA	MDH	Cit/La + Ma	La/G	G/G6P	La/Pyr	Ma/OA
SCC	1	0.59	−0.69	0.98	0.97	0.52	0.44	−0.32	0.24	0.13	0.04	−0.37	0.65	0.58	0.53	0.57	−0.48	−0.10	0.54	−0.16	0.07
		<0.001	**<0.001**	**<0.001**	**<0.001**	**0.001**	**0.007**	**0.051**	NS	NS	NS	**0.022**	**<0.001**	**<0.001**	**<0.001**	**<0.001**	**0.003**	NS	**<0.001**	NS	NS
Casein		1	−0.43	0.59	0.58	0.29	0.21	−0.28	0.25	0.09	0.09	−0.25	0.41	0.34	0.29	0.33	−0.29	−0.07	0.45	−0.07	−0.18
			0.016	**<0.001**	**<0.001**	NS	NS	NS	NS	NS	NS	NS	**0.027**	**0.051**	NS	**0.051**	NS	NS	**0.013**	NS	NS
Lactose			1	−0.69	−0.69	−0.57	−0.67	0.48	−0.27	−0.07	0.24	0.42	−0.75	−0.61	−0.72	−0.48	0.59	0.15	−0.73	0.22	0.03
				<0.001	**<0.001**	**<0.001**	**<0.001**	**0.007**	NS	NS	NS	**0.02**	**<0.001**	**<0.001**	**<0.001**	**0.008**	**<0.001**	NS	**<0.001**	NS	NS
CD18$^+$				1	1.00	0.59	0.44	−0.36	0.27	0.17	−0.01	−0.42	0.70	0.63	0.58	0.61	−0.54	−0.07	0.59	−0.24	0.08
					<0.001	**<0.001**	**0.007**	**0.028**	NS	NS	NS	**0.009**	**<0.001**	**<0.001**	**<0.001**	**<0.001**	**<0.001**	NS	**<0.001**	NS	NS
PMN					1	0.61	0.45	−0.37	0.28	0.17	−0.02	−0.44	0.71	0.65	0.60	0.63	−0.54	−0.08	0.61	−0.24	0.09
						<0.001	**0.006**	**0.024**	NS	NS	NS	**0.007**	**<0.001**	**<0.001**	**<0.001**	**<0.001**	**<0.001**	NS	**<0.001**	NS	NS
La						1	0.53	−0.39	0.63	0.39	−0.09	−0.44	0.73	0.74	0.68	0.70	−0.82	−0.09	0.52	−0.52	−0.11
							<0.001	**0.018**	**<0.001**	**0.017**	NS	**0.007**	**<0.001**	**<0.001**	**<0.001**	**<0.001**	**<0.001**	NS	**0.001**	**0.001**	NS
Ma							1	−0.40	0.42	0.10	−0.02	−0.46	0.74	0.31	0.74	0.33	−0.56	−0.07	0.66	−0.24	0.15
								0.015	**0.01**	NS	NS	**0.004**	**<0.001**	**0.05**	**<0.001**	**0.05**	**<0.001**	NS	**<0.001**	NS	NS
Cit								1	−0.19	0.19	−0.14	−0.06	−0.57	−0.41	−0.62	−0.22	0.57	0.34	−0.47	0.29	0.12
									NS	NS	NS	NS	**<0.001**	**0.012**	**<0.001**	NS	**<0.001**	**0.043**	**0.003**	**0.05**	NS
OA									1	0.49	0.07	−0.16	0.48	0.25	0.39	0.28	−0.62	0.18	0.28	−0.45	−0.28
										0.002	NS	NS	**0.003**	NS	**0.018**	NS	**<0.001**	NS	NS	**0.005**	NS
Pyr										1	−0.19	−0.22	0.13	0.31	0.01	0.41	−0.40	0.79	0.01	−0.47	−0.25
											NS	NS	NS	**0.059**	NS	**0.011**	**0.015**	**<0.001**	NS	**0.004**	NS
G6P											1	0.30	−0.07	−0.09	−0.13	−0.10	−0.05	−0.13	−0.17	−0.09	−0.33
												0.05	NS	NS	NS	NS	NS	NS	NS	NS	**0.04**
G												1	−0.57	−0.43	−0.47	−0.42	0.12	−0.05	−0.67	−0.01	−0.18
													<0.001	**0.008**	**0.003**	**0.009**	NS	NS	**<0.0001**	NS	NS
G6PD													1	0.61	0.90	0.60	−0.72	−0.12	0.83	−0.32	0.07
														<0.001	**<0.001**	**<0.001**	**<0.001**	NS	**<0.001**	**0.05**	NS
LDH														1	0.54	0.91	−0.56	−0.09	0.44	−0.30	−0.04
															<0.001	**<0.001**	**<0.001**	NS	**0.007**	**0.05**	NS
MDA															1	0.50	−0.62	−0.25	0.85	−0.25	0.13
																0.002	**<0.001**	NS	**<0.001**	NS	NS
MDH																1	−0.49	0.01	0.40	−0.29	0.05
																	0.002	NS	**0.013**	**0.05**	NS
Cit/La + Ma																	1	−0.12	−0.43	0.74	0.264
																		NS	**0.008**	**<0.001**	NS
La/G																		1	−0.14	−0.18	0.19
																			NS	NS	NS
G/G6P																			1	−0.16	0.23
																				NS	NS
La/Pyr																				1	0.48
																					0.002
Ma/OA																					1

[a] SCC – somatic cell count; PMN – polymorphonuclear; La – lactate; Ma – malate; Cit – citrate; OA – oxaloacetate; Pyr – pyruvate; G6P – glucose-6-phosphate; G – glucose; G6PD – glucose-6-phosphate dehydrogenase; LDH – lactate dehydrogenase; MDA – malondialdehyde; MDH – malate dehydrogenase.

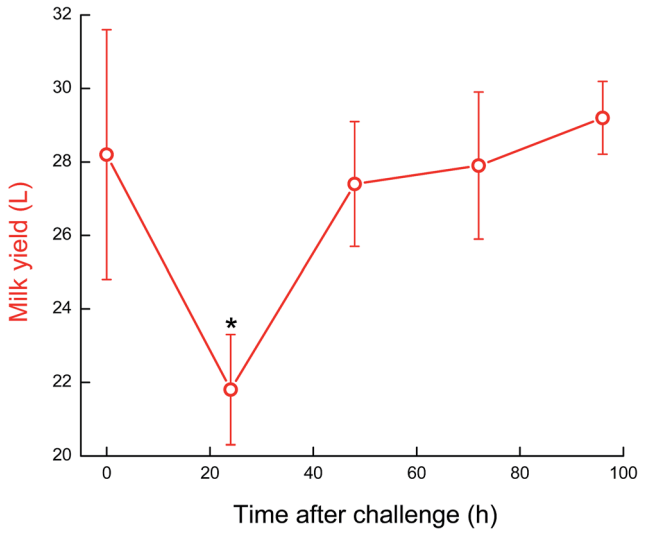

Fig. 3 Effect of challenging a single mammary gland of a cow's udder (5 cows) with lipopolysaccharide on whole cow milk yield (○) for up to 96 h. * indicates a significant difference at $P < 0.01$.

~45% in lactose concentration in the milk: from a typical concentration of ~153 mM before treatment to as low as ~94 mM between 6 to 24 h post-treatment (Fig. 4). Lactose concentration reached pre-treatment levels at 96 h. The kinetics of changes in lactose level closely followed the kinetics of the inflammatory response and was reflected by significant negative correlations with log SCC and leukocyte number (Table 1). The kinetics of changes in lactose concentration were consistent with previous studies.[12]

Effect of LPS-IMC on concentration of G and G-derived carbons in milk

The pre-treatment G concentration of ~170 μM was typical for cow's milk.[9–11] The concentration of G in milk at 3 h post-treatment increased briefly to ~480 μM (Fig. 4). However, this increase most likely reflected a brief opening of the tight junctions between MECs, which allowed penetration of G from the systemic fluid into the milk.[29] Apart from these changes, milk G concentration exhibited kinetics that closely followed that of lactose: it reached its lowest level at ~21 μM 24 h post-treatment and returned to pre-treatment levels at 72 h (Fig. 4), which was reflected by a positive correlation between milk lactose and G concentrations (Table 1). To the best of our knowledge, this is the first demonstration of the response of milk G concentration to LPS-IMC.

The pre-treatment G6P concentration of ~47 μM and G6P/G ratio of ~0.06 (Fig. 5) were consistent with previous findings in cows.[9–11] Unlike the pattern of G changes, G6P concentration increased to ~70 μM at 6 h post-treatment under LPS-IMC, and then fluctuated around its pre-treatment concentration until the end of the experiment (Fig. 5). Consequently, the G6P/G ratio was 4.3 at 24 h post-treatment, 0.8 at 48 h post-treatment, and only returned to its pre-treatment level at 96 h post-treatment (Fig. 5). A similar increase in G6P/G ratio to >1 has been recorded in early lactating cows, a period characterized by negative energy balance associated with massive lipolysis and increased oxidative stress.[11]

Pyruvate concentration in the pre-treated cows (~13 μM) was somewhat lower than that found in beef breeds at various stages of lactation (20–40 μM).[30] This is probably related to the much higher milk yield. Hence, metabolic rate in the lactating cows was used here. This is the first study (to the best of our knowledge) in which the concentration of Pyr was reported and methodologically followed in response to LPS-IMC (Fig. 6). Challenge induced a sharp increase in Pyr concentration to ~439 μM at 12 h post-treatment, which most likely reflects an abrupt arrest of Pyr supply to the mitochondria. Pyr concentration did not return to its pre-treatment levels and between 24 h and 96 h post-treatment it fluctuated around 400 μM.

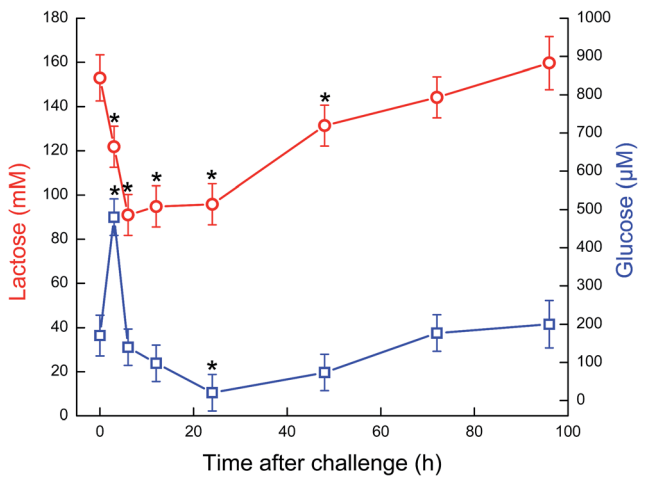

Fig. 4 Effect of challenging a single mammary gland of a cow's udder (5 cows) with lipopolysaccharide on the ontogenesis of lactose (○) and glucose (□) concentration for up to 96 h. * indicates a significant difference at $P < 0.01$.

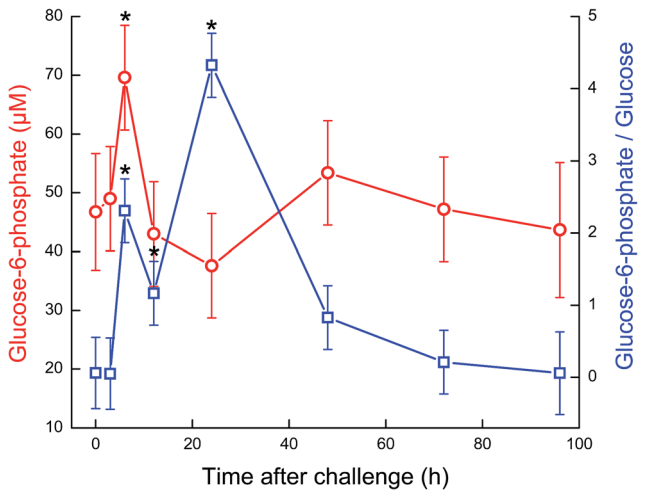

Fig. 5 Effect of challenging a single mammary gland of a cow's udder (5 cows) with lipopolysaccharide on the ontogenesis of glucose-6-phosphate concentration (○) and the ratio between glucose-6-phosphate and glucose (□) for up to 96 h. * indicates a significant difference at $P < 0.01$.

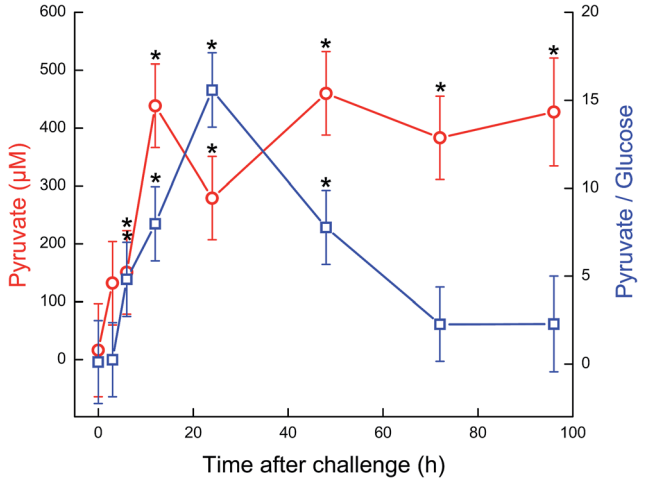

Fig. 6 Effect of challenging a single mammary gland of a cow's udder (5 cows) with lipopolysaccharide on the ontogenesis of pyruvate concentration (○) and pyruvate/glucose ratio (□) for up to 96 h. * indicates a significant difference at $P < 0.01$.

Consequently, the ratio between Pyr and G increased substantially after LPS-IMC (Fig. 6).

In cow's milk, La concentration increases when the mammary gland is inflamed.[10] Following LPS-IMC, a sharp transient increase in milk La concentration was found.[12] Consistent with those reports, La concentration increased from ~64 μM in pre-treated cows to ~1100 μM at 12 and 24 h post-treatment, and then dropped to ~611 μM at 96 h post-treatment (Fig. 7).

Highly significant correlations between La concentration and log SCC, leukocyte number and MDA concentration were found (Table 1). A La/G ratio of ~0.5 before LPS-IMC most likely reflected the small proportion of La formation from the G that enters the MEC (Fig. 7). The sharp increase in La/G ratio to 30–56 between 6 and 24 h post-treatment most likely reflects the abrupt conversion of MEC to AG and the reduction of the La/G ratio to 3.1 at 96 h, suggesting that the treated mammary gland metabolism sustains a higher proportion of AG than before the treatment (Fig. 7). The La/Pyr ratio approximately reflects the redox state in the MEC cytosol (see Discussion). LPS-IMC induced a reduction in the La/Pyr ratio and despite two peaks at 6 & 24 h; this ratio remained low until the end of the study (Fig. 8).

Previous reports from our laboratory have shown that Ma concentration in cow's milk responds acutely to LPS-IMC,[12] bacterial infection[10] and induction of involution.[13] Consistent with these previous studies, LPS-IMC induced a sharp increase in Ma concentration,[12] which paralleled the changes in La concentration, although the concentration of Ma at peak levels (~2000 μM at 6 h and 48 h post-treatment) exceeded that of La (Fig. 9). In contrast to the behavior of La, the concentration of Ma returned to its pre-treatment level within 96 h. The rather similar behavior of Ma and La concentrations in response to LPS-IMC was reflected by highly significant correlations between Ma and La concentrations and between Ma concentration and log SCC, leukocyte number and MDA concentration, and by significant inverse correlations with lactose and G (Table 1). The Ma/OA ratio was >3 until 72 h post-treatment and dropped to <2 thereafter (Fig. 8).

The present study is the first to monitor changes in OA concentration in milk following LPS-IMC. The pre-treatment level of OA was relatively low (~132 μM). At 3 h after LPS-IMC, OA concentration rose to ~660 μM and between 6 and 96 h post-treatment, OA concentrations ranged between 800 to 1000 μM (Fig. 9).

Pre-treatment Cit concentration was ~10 mM. LPS-IMC induced a rapid decrease in Cit concentration, reaching a nadir of ~3.8 mM at 6 h post-treatment and returning to the pre-treatment level at 48 h post-treatment (Fig. 10). The kinetics of Cit changes were inversely related to changes in La and Ma

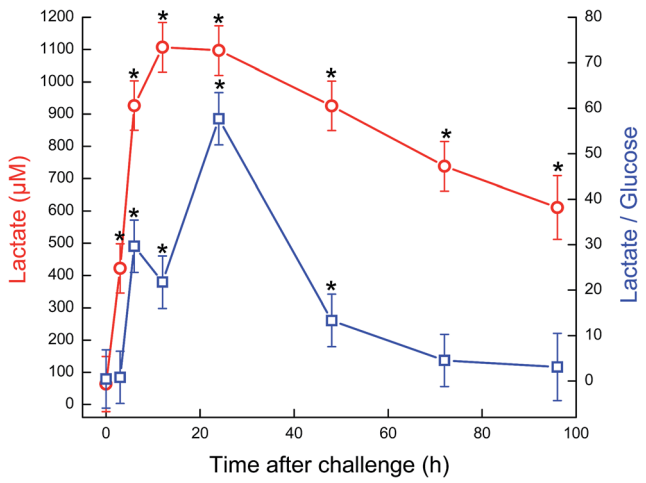

Fig. 7 Effect of challenging a single mammary gland of a cow's udder (5 cows) with lipopolysaccharide on the ontogenesis of lactate (○) and lactate/glucose ratio (□) for up to 96 h. * indicates a significant difference at $P < 0.01$.

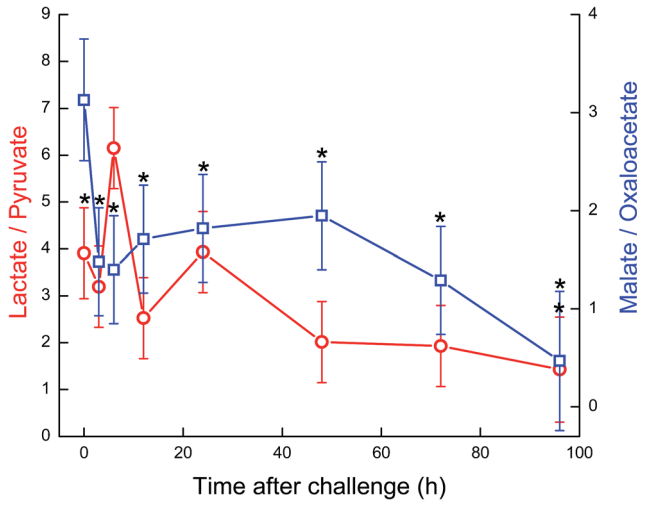

Fig. 8 Effect of challenging a single mammary gland of a cow's udder (5 cows) with lipopolysaccharide on the ratio between lactate/pyruvate (○) and between malate/oxaloacetate (□) for up to 96 h. * indicates a significant difference at $P < 0.01$.

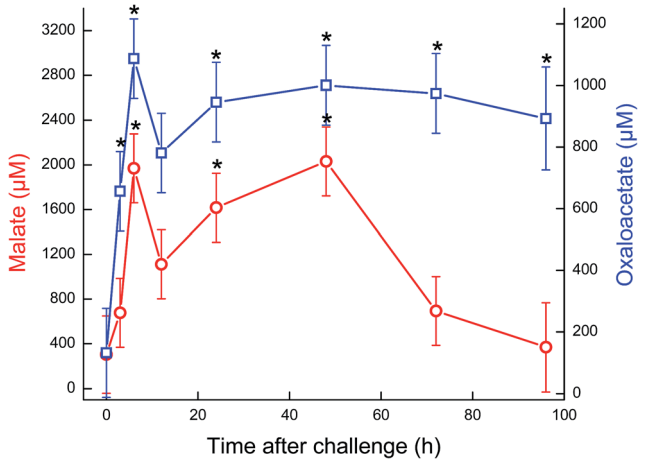

Fig. 9 Effect of challenging a single mammary gland of a cow's udder (5 cows) with lipopolysaccharide on the concentration of malate (○) and oxaloacetate (□) for up to 96 h. * indicates a significant difference at $P < 0.01$.

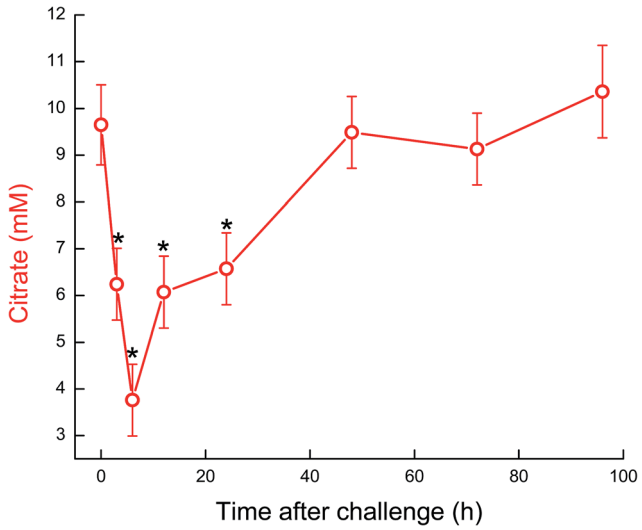

Fig. 10 Effect of challenging a single mammary gland of a cow's udder (5 cows) with lipopolysaccharide on the concentration of citrate (○) for up to 96 h. * indicates a significant difference at $P < 0.01$.

concentrations. Consequently, Cit concentration was negatively correlated with La and Ma concentrations, log SCC, leukocyte number and MDA concentration, whereas it was positively correlated with lactose and Pyr concentrations (Table 1).

Effect of LPS-IMC on key NAD^+/P^+-dependent enzymes

G6PD activity pre-treatment was ~9 mU mL^{-1}. After LPS-IMC, its activity increased rapidly with kinetics resembling those of other inflammatory responses (*e.g.*, log SCC and La concentration), reaching a peak of ~82 mU mL^{-1} at 24 h post-treatment. Then, G6PD activity declined and at 96 h post-treatment, its activity fell to the pre-treatment level (~12 mU mL^{-1}; Fig. 11). Consequently, G6PD activity was significantly and positively correlated with SCC, leukocyte number (PMN), LDH activity,

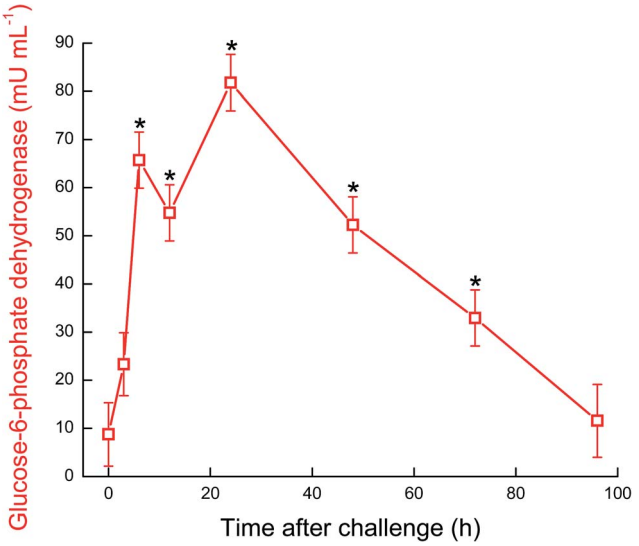

Fig. 11 Effect of challenging a single mammary gland of a cow's udder (5 cows) with lipopolysaccharide on the activity of glucose-6-phosphate dehydrogenase (○) for up to 96 h. * indicates a significant difference at $P < 0.01$.

MDH activity and the concentrations of G6P, La, Ma and OA in milk. G6PD activity was significantly and negatively correlated with the concentrations of lactose, G and Cit (Table 1).

MDH activity in milk closely reflects MDH activity in the cytosol of MECs,[31] as recently verified.[11] MDH activity pre-treatment was ~70 mU mL^{-1}. After LPS-IMC, its activity increased rapidly with kinetics resembling those of other inflammatory responses (*e.g.*, log SCC and La concentration), reaching a peak of ~3700 mU mL^{-1} at 24 h post-treatment. Then, MDH activity declined and at 96 h post-treatment, its activity fell to ~250 mU mL^{-1} (Fig. 12). MDH activity was significantly and positively correlated with log SCC, leukocyte number, the activities of G6PD and LDH and the concentrations of MDA, La, Ma and Pyr in milk. MDH activity was significantly

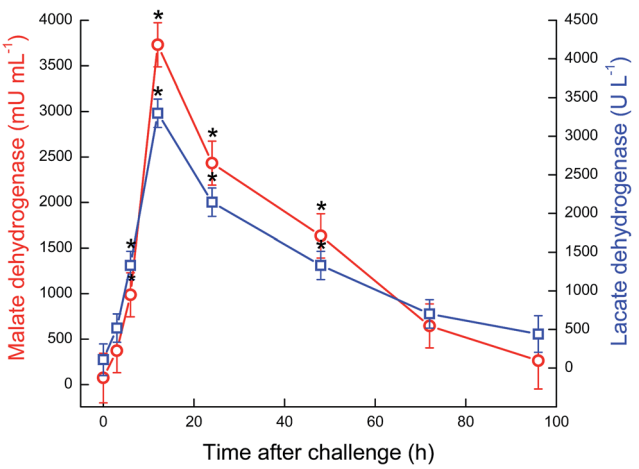

Fig. 12 Effect of challenging a single mammary gland of a cow's udder (5 cows) with lipopolysaccharide on the activities of malate dehydrogenase (○) and lactate dehydrogenase (□) for up to 96 h. * indicates a significant difference at $P < 0.01$.

and negatively correlated with the concentrations of lactose and G (Table 1).

Pre-treatment LDH activity was ~107 U L^{-1}. After LPS-IMC, its activity increased rapidly with kinetics resembling those of other inflammatory responses (*e.g.*, log SCC and La concentration), reaching a peak of ~3300 U L^{-1} at 12 h post-treatment and then declining. However, as with La concentration, LDH activity at 96 h post-treatment remained higher than its pre-treatment level (440 U L^{-1}) (Fig. 12). LDH activity was significantly and positively correlated with SCC, leukocyte number, the activities of MDH and G6PD and the concentrations of MDA, La and Ma in milk. LDH activity was significantly and negatively correlated with the concentrations of lactose, G and Cit (Table 1).

Discussion

Pros and cons in our experimental approach

The close correlations between relevant metabolites and their patterns firmly support the concept that the concentration of G and G-derived carbons in milk mirror the major activities of those metabolites in the PPP and glycolytic pathway in the MEC cytosol. Equivalent information can only be obtained by working *in vitro* or *in situ* on MEC lines and explants.[32] These latter techniques are advantageous over the methodology used in this report in providing relevant information on signal transduction, and molecular and genomic events in MECs. However, to study some cellular functions, primary cultures of freshly isolated cells are often preferred, since established cell lines do not always express specialized properties in culture.[33] The metabolic activity of MECs under such conditions merely reflects the *in vivo* metabolic rate in milk-producing animals; for instance, casein synthesis in the picogram per gram range per 4 h in explants obtained from mammary gland biopsies[33] is 4 logarithmic scales lower than the *in vivo* synthesis/secretion rate of casein at 0.8 g g^{-1} per 4 h (as calculated from the *in vivo* pre-treatment values and assuming that secretion is about equal to synthesis). As elaborated below, the effect of LPS on whole-body metabolism is critical for understanding why the shift of MECs to AG is a basic homeostatic response. Some of the above-noted drawback is compensated for by the fact that LPS has been used extensively as a model to induce inflammation in mammary glands in mice[34,35] and dairy cows.[35,36] Consequently, there is a relative wealth of information from this technique, which can be used to support concepts derived from the results of this study. It is well known that G easily passes through membrane channels into milk, and that its concentration in milk reflects the G concentration in the MEC cytosol. It is also well established that many cellular metabolites, such as La[12] and β-hydroxybutyrate,[37] easily pass through channels in the plasma membrane of MECs. The present results strongly suggest that the concentrations of G6P, La, Ma, OA and Pyr in milk also directly reflect their concentrations in the MEC cytosol.

LPS-IMC induces a tradeoff between the use of G by MECs and the immune system

Inflammation of mammary glands due to bacterial infection with pathogens such as *Staphylococcus aureus*, coagulase-negative staphylococci and *E. coli* induces a decrease in milk yield and compositional changes in the milk, particularly with respect to lactose concentration. In ruminants (goat, sheep and cows), mammary inflammation causes a decrease in the concentration and total yield of lactose in milk, and consequently there is an increase in milk's fat and protein levels.[19,38–40] Milk volume is dictated by lactose secretion because lactose is its main osmotic component.[41] Thus, understanding the importance of the sharp reduction in lactose secretion during inflammation is a key to understanding the physiological basis of this response. The reduction in lactose concentration is specific to the affected gland, whereas the percentages of fat and protein in milk do not differ between infected and uninfected glands.[10,16,38,39]

Milk secretion is controlled by negative-feedback signals that are induced by milk stasis.[38,39,42] Since the cows were continually milked during the experiment, the reduction in milk yield is not trivial and has to be accounted for by a specific response. As discussed herein, this response is the conversion of MEC metabolism to predominantly AG.

The acute inflammatory response in this study was consistent with many other descriptions[12,28,34,36] and was associated with an acute increase (within 6 h) in the number of leukocytes in milk, from hundreds of thousands per mL to tens of millions or more per mL. Such an acute immune response requires a considerable proportion of whole-body G resources.[16] Cells that rely primarily on G for energy are members of the central nervous system, red blood cells and cells composing the innate immune system.[43] In severely septic human patients, energy expenditure increases by ~50%.[44] This acute demand for G is made shortly after the LPS challenge and therefore relies on existing body resources. In the present experiment, and consistent with previous results,[12] at peak of the response (milk production of ~28 L day^{-1} 24 and 48 h post-treatment) there was a reduction of ~250 g lactose per day secreted from the treated gland. As G is the only source for lactose (either directly or through conversion of G to UDP-galactose synthesis in the mammary gland),[14] and as each molecule of lactose is built of 2 molecules of G, the acute reduction in lactose synthesis prevented the extraction of ~500 g G from the blood in the treated gland (Fig. 13). Thus, our results suggest that LPS-IMC induces a massive decrease in the demand for G in the challenged gland. The shift of MECs to predominantly AG enables a drastic reduction in the treated mammary glands use of G, which is liberated to support the massive flow of leukocytes to that gland. The reduction in food intake under LPS challenge is much smaller than the reduction in milk yield, as clearly demonstrated by Waldron *et al.*[45] LPS-induced experimental mastitis in dairy cows provokes an increase in G production and plasma G concentration.[45] The maintenance of high G production despite the dramatic decrease in G usage by the mammary gland suggests that the LPS-induced conservation of G is a protective mechanism, which allows for an effective immune response early in *E. coli* invasion of the mammary gland.[12] Additional advantages are derived from the fact that reduced lactose concentration and increased La and Ma concentration impair the growth of *E. coli* in milk.[12]

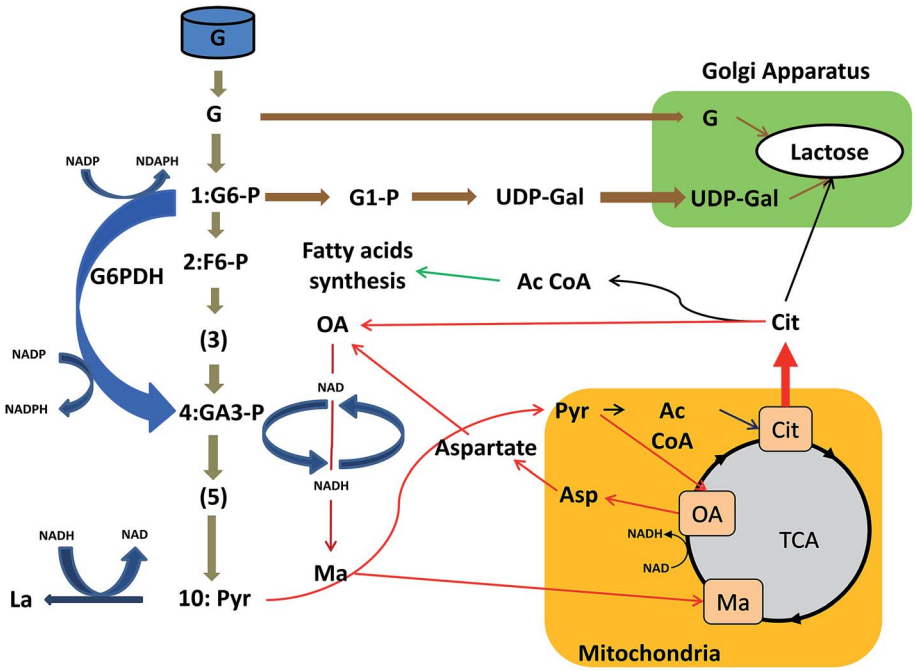

Fig. 13 Schematic illustration of metabolic pathways associated with homeostatic aerobic glycolysis. Glycolysis axis is marked in grey. Pentose phosphate pathway is marked in blue. Metabolic pathways of lactose synthesis are marked in brown. Transhydrogenation pathways between the mitochondria and the cytosol are marked in red (see text for further explanations). Abbreviations: G – glucose; G6-P – glucose-6-phosphate; G1-P – glucose-1-phosphate; UDP-Gal – uridine diphosphate galactose; F6P – fructose-6-phosphate; GA3-P – glyceraldehyde triphosphate; TCA – tricarboxylic acid; Cit – citrate; La – lactate; Ma – malate; Pyr – pyruvate; Asp – aspartate; Ac CoA – acetyl coenzyme A.

LPS-IMC induces the flow of G6P through the PPP

In most cells, the entering G is rapidly phosphorylated by hexokinase because most uses of G for cellular biochemical tasks require its phosphorylation. Hence, in cow's milk and MECs, the typical G6P/G ratio is 0.3–0.5 [9,11,14] (Fig. 5: pre-treatment values), which likely reflects the need for free G for lactose synthesis. Thus, we assume that this ratio will vary among mammalian MECs according to the lactose level in their milk.

As G6P is derived from G, the only possible explanation for a G6P/G ratio >1, as found here at the peak of the inflammatory response following LPS-IMC, is blockage of G flow downstream along the glycolysis pathway or its recycling from cytosolic G-derived carbons, such as fructose-6-phosphate.[46] The increase in G6P concentration likely brings it closer to the optimal K_m of G6PD and together with the increase in G6PD activity, shunts G6P through the PPP.[11] This shift to the PPP results in the production of 2 molecules of NADP per molecule of G6P. Conversion of oxidized glutathione to reduced glutathione by glutathione reductase is a central reaction in the degradation of H_2O_2. This reaction requires NADP as a cofactor, thereby increasing the cell's requirement for NADP during oxidative stress.[46]

Early lactation in dairy cows is associated with oxidative stress resulting from extensive lipolysis as a result of negative energy balance.[11] The significant correlations between milk G6PD activity and the G6P/G ratio, and G6PD activity and MDA concentration in early lactation and following LPS challenge, suggest that G6P is shunted to the PPP in the mammary gland as part of homeostatic adaptations to oxidative stress. Thus, Zachut *et al.*[11] and our data highlight the potential of using measurements of milk G6P/G ratio as an objective, accurate and noninvasive technique to evaluate exposure to oxidative stress in lactating cows and potentially other mammals.

Consistent with our hypothesis, it is known that PPP regulation during the oxidative-stress response is a conserved paradigm from yeast to mammals of the cellular antioxidant defense mechanism *via* reduction of $NADP^+$ to NADPH.[46] Interestingly, it becomes clearer that the PPP plays a critical role in regulating cancer cell growth by supplying cells with not only ribose-5-phosphate (for reductive biosynthesis and ribose biogenesis) but also NADP for detoxification of intracellular reactive oxygen species.[47] Thus, increased flow of G-derived carbons through the PPP and the conversion to AG are common features of the regulatory response to oxidative stress and the Warburg effect in cancer cells. However, as discussed below, there is a difference between the two.

LPS-IMC induces MEC shift to AG

LPS-IMC rapidly induced a shift in MEC metabolism to AG, as reflected by the sharp increase in La concentration, La/Pyr ratio and La/G ratio. However, the physiological features of AG induced by LPS challenge were fundamentally different from the Warburg effect in cancer cells: cancer cells produce energy predominantly *via* a high rate of glycolysis in conjunction with a high rate of La production, rather than by a comparatively low rate of glycolysis followed by oxidation of Pyr in the mitochondria and formation of most of the cell energy by OxPhos

reactions, as in most normal cells. Metabolic conversion to AG in cancer cells is a result of reduced mitochondrial activity.[1]

In our study, the immediate sharp increase in Pyr concentration following LPS-IMC suggested that the shift to AG is a consequence of blocked entrance of Pyr into the mitochondria. Our methodology could not reveal the mechanism underlying that response; however, there is a wealth of information supporting this assumption. HIF-1 is a heterodimeric transcription factor that functions as a master regulator of oxygen homeostasis in all metazoan species.[48] The acute inflammatory response induced by LPS-IMC induces activation of the NF-κB pathway in exposed cells, including MECs.[49] TNF-α, a cytokine induced by LPS challenge,[35] and NF-κB transcriptionally upregulate HIF-1 formation and upregulating LDH activity. HIF-1 actively suppresses metabolism through the tricarboxylic acid (TCA) cycle by directly transactivating the gene encoding pyruvate dehydrogenase kinase 1 (PDK1).[48] PDK1 inactivates the TCA cycle enzyme pyruvate dehydrogenase, which converts pyruvate to acetyl-CoA and thus, under LPS challenge, prevents the formation of Cit which initiates the TCA cycle.

In contrast to increased extraction of G by cancer cells, LPS-IMC induced a sharp decrease in G extraction from the blood, as reflected by the sharp reduction in lactose synthesis and secretion and the sharp reduction in G concentration at the peak of the response. Blood flow to organs, including the mammary glands, is autoregulated by metabolic rate of cells in that organ.[50,51] The ~40% reduction in the concentration of Cit, which directly reflects the concentration of metabolites in the TCA cycle (Fig. 14a and b) suggested a similar drop in ATP production by OxPhos. Thus, the sharp reduction in ATP production and consequently in oxygen consumption by MECs in response to the shift to AG explains the sharp reduction in G extraction from the blood. As discussed above and presented schematically in Fig. 14a and b, the shift to AG allows diverting G to support the innate immune system. Thus, the shift of MECs to AG as part of the acute immune response may be defined as homeostatic AG (HAG).

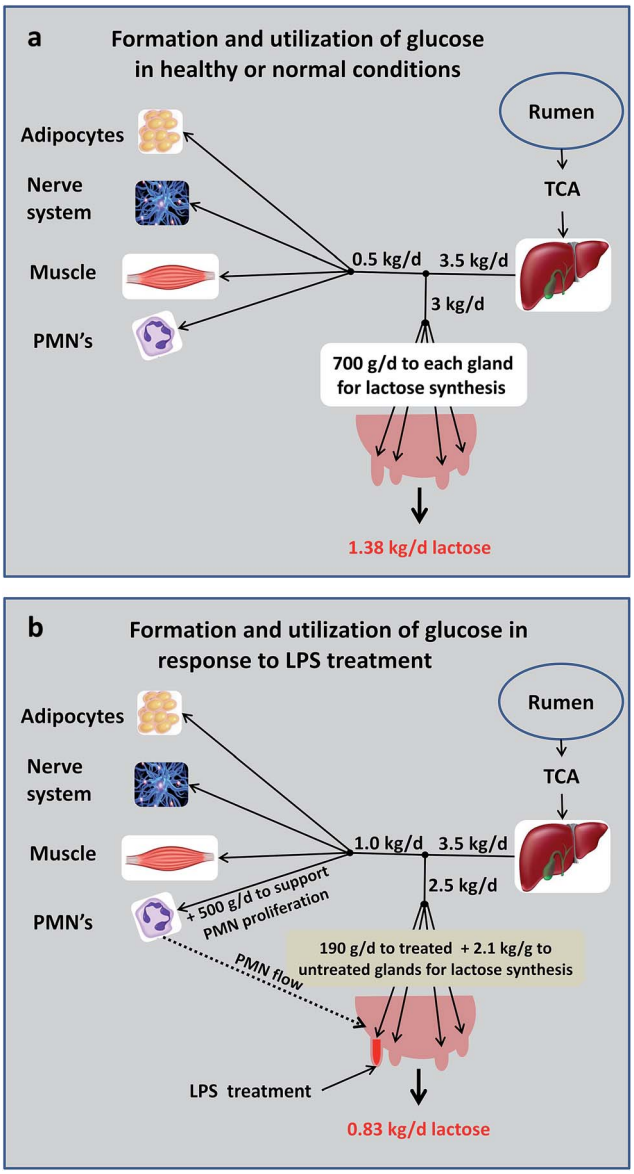

Fig. 14 Schematic illustration of glucose balance in the mammary gland upon activation of homeostatic aerobic glycolysis. Panel a: Non-stresses schematic presentation of the whole body glucose metabolism is presented. In ruminants, most glucose is derived from gluconeogenesis in the liver. Extraction of glucose by the mammary glands was calculated based on lactose output in milk (a product of milk yield and milk lactose concentration) and that two molecules of glucose are required to synthesize one molecule of lactose. Whole body glucose entry rate was calculated based on the assumption that the mammary glands extract 0.8 of the glucose released from the liver and the use of glucose by non-mammary tissues was calculated as the difference between whole body glucose entry rate and extraction of glucose by the mammary glands. PMN – polymorphonuclear, TCA – tricarboxylic acid. Panel b: The effect of lipopolysaccharide (LPS) challenging of a single mammary gland on glucose utilization is schematically illustrated. It is assumed that the whole body glucose entry rate remained similar. Reduction of glucose extraction by the treated gland was calculated based on the reduction of lactose output in the treated gland, as explained above. It is assumed that the saved glucose is used to support the massive flow of PMN's to the treated gland (see text for further explanations). PMN – polymorphonuclear, TCA – tricarboxylic acid.

LPS-IMC induces homeostatic responses to maintain the redox balance in the cytosol

The coenzyme NAD is a key electron carrier that mediates hundreds of enzymatic reactions. The redox state of NAD^+/NADH-coupled reactions plays a central role in energy metabolism.[52] The NAD^+/NADH ratio has also been shown to be involved in metabolic disorders, oxidative stress, cell ageing, signal transduction and transcriptional regulation. NAD^+ and NADH are present in the different cell compartments and their distribution is uneven. In addition to the free species, NAD^+ and especially NADH are partly present in protein-bound forms.[53,54] Thus, measurements of whole-cell total concentrations of NAD^+ and NADH do not distinguish between different compartments' pools or between free and protein-bound forms, so they provide no information on the *in vivo* redox state of the NAD^+/NADH couple inside the cell compartments.[55,56] These limitations can be overcome by calculating the NAD^+/NADH ratio from the

concentrations of oxidized and reduced reactants of suitable near-equilibrium reactions:[55]

$$\frac{NAD^+}{NADH} + H^+ = (\sim)[\text{oxidized product}] / [\text{reduced substrate}]K' \text{ eq} \quad (2)$$

where K' eq is the reaction constant at near-equilibrium.

In mammalian cells, the NAD^+/NADH ratio in the cytosol can be determined from the La/Pyr ratio in the cytosol.[55,56] Here, we used milk's particular attribute of directly reflecting the level of G-derived carbons in the MEC cytosol to evaluate how the shift to AG is reflected in the evolution of the NAD^+/NADH ratio in the affected MECs. The initial La/Pyr ratio of ~5.4 (Fig. 8) found here was lower than the ratio of ~12 found in the cytosol of rat liver cells and thus NAD^+/NADH was likely much lower than the ratio of ~700 found in rat liver.[55] To the best of our knowledge, there are no data in the literature supporting or negating this conclusion. Induction of inflammatory stress with LPS induced a sharp reduction in La/Pyr–NAD^+/NADH ratio, despite the transient restoration of the NAD^+/NADH ratio at 6 and 12 h post-treatment (Fig. 8). The NAD^+/NADH ratio remained 2.8- to 3.8-fold lower than the initial level at the end of the study, suggesting that full recovery of the La/Pyr redox state of MECs occurs at later stages. Unlike in cancer cells experiencing the Warburg effect,[1] the conversion of La into Pyr with simultaneous conversion of NADH to NAD^+ is not sufficient to maintain a high NAD/NADH ratio.

Our results suggest that the Ma–Asp shuttle is also activated as a mechanism to restore the NAD^+/NADH ratio in the cytosol. At any given time point, mitochondria contain high concentrations of TCA components. In addition, Cit cycling in the TCA cycle was not completely blocked following LPS-IMC, as judged by the fact that Cit concentration was only reduced by 40%. Thus, the mitochondria could still serve as a source of hydrogen for the oxidation of NADH to NAD^+:

$$NADH + H^+ \Rightarrow NAD^+ + 2H^+ + 2e^- \quad (3)$$

($NADH$ loses e^-, the oxidation half of the reaction).

Transhydrogenation by the Ma–Asp shuttle is carried out by exporting Asp from the mitochondria to the cytosol where it is converted by aspartate transaminase in the presence of α-ketoglutarate to OA + glutamate. OA is converted by MDH-subtype 1 to Ma with simultaneous conversion of NADH to NAD^+:

$$OA + 2H^+ + 2e^- \Rightarrow \text{Ma (Ma gains } e^-\text{, the reductive half of the reaction)} \quad (4)$$

The positive Ma/OA ratio that prevailed throughout most of the experiment (from pre-treatment to 48 h post-treatment) is consistent, according to eqn (2), with a reduction of OA to Ma (Fig. 13) and simultaneous oxidation of NADH to NAD^+. From 72–96 h post-treatment, this ratio, unlike that of La/Pyr, dropped to below 1, which is consistent with the reduction of Ma concentration to pre-treatment levels; it suggests other uses of cytosolic OA, such as conversion into Asp for anabolic amino acid synthesis.

The sharp increase in Ma concentration at 3–48 h post-treatment strongly suggests that its passage into the mitochondria is blocked under inflammatory stress. Thus, for transhydrogenation, instead of recycling Ma into the mitochondria where it is incorporated into the TCA cycle for production of NADH, it is released into the milk. The release of Ma into milk likely occurs through the same channels used for La release.

The simultaneous oxidation–reduction reactions in converting Pyr to La and OA to Ma (*i.e.*, eqn (3) and (4)) are typical to redox reactions, and they neutralize the H^+ formed during those reactions. The secretion of Ma and La into milk in their protonated forms prevents the reduction of cell pH due to accumulation of those weak acids in the cytosol. In turn, accumulation of protonated La and Ma in the millimolar range in milk has been shown to contribute to the development of a bacteriostatic response to pathogenic *E. coli*. The decrease of lactose concentration in milk delays the growth of pathogenic *E. coli*, which must use lactose anaerobically to grow in milk.[12] Thus, in addition to liberation of G to support the immune system, HAG in MECs under inflammation contributes to the innate defense mechanisms against bacterial invasion.

In most of our studies carried out under acute inflammation, acute involution or chronic inflammation,[10,13] (Fig. 9), the increase in Ma due to the MEC shift to AG was greater than that of La, suggesting that formation of Ma is even more important than formation of La in restoring the redox state in the cytosol of affected cells. No equivalent information is available and the potential importance of our finding is discussed below.

On the common features of responses to hypoxia (Pasteur effect), inflammation and HAG

The response to hypoxic environment, classically induced by low ambient oxygen, and the innate system that is forcefully activated by substances such as LPS, are ancient stress responses that share common features, such activation of common signal-transduction pathways and similar effectors, such as the release of similar cytokines. Specifically, these two systems are interrelated through their induced transcription factors.[57] NF-κB and activation of the HIF-1 signal-transduction pathway are central responses to hypoxia. However, LPS challenge induces the NF-κB signal pathway and in particular, an increase in the activity of the kinase IKK-b, which raises the level of the transcriptional regulator of HIF-1 in macrophages and decreases prolyl hydroxylase mRNA production in a toll-like receptor 4 (TLR4)-dependent fashion.[57] For instance, deletion of HIF-1 in macrophages was found to be protective against LPS-induced mortality (sepsis) and to block the development of clinical markers, including hypotension and hypothermia.[58]

However, one might also assume that the relationship between the common activation of these two systems has evolutionary advantages, related to improved resistance to infection and stressful conditions. Adaptation to hypoxia was important in early stages of evolution when life developed under the relatively hypoxic conditions of the ancient sea. After adaptation to terrestrial life, hypoxia became much less

significant for most organisms. It is possible that HAG is an energy-saving mechanism that was adapted for use in multicellular organisms under stressful conditions for more efficient allocation of G in situations where G is critically required by certain types of cells (innate immune system) or organs (central nervous system) for the organism's survival.

Hypoxia is generally considered a side effect of inflammation,[57] and inflammation can cause localized hypoxia (*e.g.*, following vaso-occlusion under stroke and heart failure or in diabetic wounds). However, as inflammation is typically associated with increased blood flow to the infected site, hypoxia as a side effect of inflammation can hardly be considered a general phenomenon. In the present study we showed that LPS-IMC induces a shift toward AG at the expense of mitochondrial metabolism under *in vivo* conditions without restricting oxygen supply to the glands. Moreover, release of a large quantity of La from sites of sepsis and inflammation in animal models and from human blood have been related to La's release as a product of glycolysis that was induced by inflammation rather than as a marker of tissue hypoxia.[59,60]

Whereas La is widely considered in diagnosis and treatment in situations such as hypoxia (*e.g.*, ischemia of the heart and brain), metabolic acidosis, acute inflammation and sepsis,[59,60] scarce information is available on the potential benefits of measuring Ma levels in systemic fluids for diagnostic purposes. Nevertheless, some reports were found to be in line with the concept of HAG being a general homeostatic response and of Ma being of diagnostic value in relevant situations. For instance, increased plasma Ma concentration was even more predictive than increased La in serial metabolite analysis following induction of hypoxic-ischemic encephalopathy in a newborn nonhuman primate model[61] and in patients with metabolic acidosis.[62] An increase in Ma levels in patients with metabolic acidosis is particularly interesting as it is obviously not associated with lack of oxygen supply to the tissues.

On the potential relationship between HAG and the reverse Warburg effect in tumors

As already noted, HAG differs from the Warburg effect in cancer cells primarily because the conversion to AG in HAG is associated with reduced utilization of G and OxPhos activity in the mitochondria, whereas the Warburg effect is characterized by increased utilization of G by cells. We cannot speculate at this stage on any cause-and-effect relationship between HAG and the Warburg effect.

However, AG may also occur in the stromal compartment surrounding cancer cells in tumors, a phenomenon that has been termed 'reverse Warburg effect'.[63] Recent studies on human tumors, including breast, prostate and head and neck cancers and lymphomas, have revealed metabolic coupling between catabolic fibroblasts and anabolic cancer cells.[63–65] The shift of cancer-associated fibroblasts to AG was found to be secondary to stress arising from reactive oxygen species *via* HIF1-α and NF-κB signaling.[63–65] La and other glycolytic metabolites that are released from the cancer-associated fibroblasts are used as energy sources by the cancerous cells. According to the reverse Warburg effect concept: "cancer should be viewed more as a systemic disease, that engages the host-organism in various forms of energy-transfer and metabolic co-operation across a whole-body 'ecosystem'".[65] This view shares common features with the HAG concept presented here. It is possible that cancer cells make use of a basic homeostatic response of many types of somatic cells in order to enslave them, thereby nourishing themselves with nutrients while they are protected deep in the tumor, far from the blood supply and contact with the immune system. Currently, demonstration of the shift of tumor somatic cells to AG is based on complicated measures of specific signal transduction and regulatory molecules from tumors biopsies, which are too complicated for practical medical diagnose.[63–65] If the shift of tumor somatic cells to AG is part of a basic homeostatic response to inflammatory oxidative stress, then the findings from the present study may lead to a breakthrough in defining the reverse Warburg effect in tumors by simple measures, such as Ma level in tumor tissue and perhaps also in relevant systemic fluids.

Conclusions

The main concepts that can be derived from the present results are: (i) LPS shifts MECs to AG as a tradeoff between use of G to support lactose synthesis and liberation of G to support the immune system. (ii) Induction of AG in MECs allows conservation of G, which is associated with an acute reduction of G drainage from the blood. (iii) Induction of AG in MECs is associated with increased flow of G6P through the PPP to support the cells' antioxidative capacity. (iv) Strong induction of AG is likely in response to acute reduction of Pyr movement from the cytosol to the mitochondria and parallel acute conversion of Pyr to La. (v) The sharp reduction in La/Pyr ratio reflects the conversion of a relatively high NAD^+/NADH ratio to a much lower one, and this response induces metabolic responses that will shift AG back to the predominant OxPhos state. (vi) The transhydrogenation loop (Fig. 13), which is based on the Ma–Asp shuttle components, but with a shunt for recycling Ma into the mitochondria, plays an important role in restoring the redox state (NAD^+/NADH ratio) of MECs. This response explains why the increase in Ma concentration in milk in response to LPS-IMC challenge is higher than the increase in La concentration.

Conflict of interest

Competing Interests Statement: the authors declare no competing interests.

Acknowledgements

The authors would like to thank Mr. Shamay Jacoby, head of the A.R.O. experimental farm and the dairy farm stuff for their valuable help in carrying out this study.

References

1 R. A. Gatenby and R. J. Gillies, *Nat. Rev. Cancer*, 2004, **4**, 891–899.
2 O. Warburg, *Science*, 1956, **123**, 309–314.
3 P. G. Arthur, P. E. Hartmann and M. Smith, *J. Pediatr. Gastroenterol. Nutr.*, 1987, **6**, 758–763.
4 M. C. Neville, W. W. Hay and P. Fennessey, *Protoplasma*, 1990, **159**, 118–128.
5 N. J. Kuhn and A. White, *Biochem. J.*, 1975, **152**, 153–155.
6 C. S. Atwood, J. K. Toussaint and P. E. Hartmann, *J. Dairy Res.*, 1995, **62**, 207–220.
7 A. Faulkner, D. R. Blatchford and H. T. Pollock, *Biochem. Soc. Trans.*, 1985, **13**, 689–690.
8 M. Peaker and A. Faulkner, *Proc. Nutr. Soc.*, 1983, **42**, 419–425.
9 T. Larsen and K. M. Moyes, *Animal*, 2015, **9**, 86–93.
10 N. Silanikove, U. Merin and G. Leitner, *J. Dairy Res.*, 2014a, **81**, 358–363.
11 M. Zachut, G. Kra, F. Portnik, F. Shapiro and N. Silanikove, *RSC Adv.*, 2016, **6**, 65412–65417.
12 N. Silanikove, A. Rauch-Cohen, F. Shapiro, S. Blum, A. Arieli and G. Leitner, *J. Dairy Sci.*, 2011, **94**, 4468–4475.
13 N. Silanikove, U. Merin, F. Shapiro and G. Leitner, *J. Dairy Sci.*, 2013, **96**, 6400–6411.
14 F. Q. Zhao, *J. Mammary Gland Biol. Neoplasia*, 2014, **19**, 3–17.
15 C. T. Kadzere, M. R. Murphy, N. Silanikove and E. Maltz, *Livest. Prod. Sci.*, 2002, **77**, 59–91.
16 D. J. Kominsky, E. L. Campbell and S. P. Colgan, *J. Immunol.*, 2010, **184**, 4062–4068.
17 P. A. Kramer, S. Ravi, B. Chacko, M. S. Johnson and V. M. Darley-Usmar, *Redox Biol.*, 2014, **2**, 206–210.
18 N. Silanikove, *Livest. Prod. Sci.*, 2000, **67**, 1–18.
19 G. Leitner, O. Krifucks, U. Merin, Y. Lavi and N. Silanikove, *Int. Dairy J.*, 2006, **16**, 648–654.
20 G. Leitner, R. Eligulashvily, O. Krifucks, S. Perl and A. Saran, *J. Vet. Med., Ser. B*, 2003, **50**, 45–52.
21 N. Silanikove and F. Shapiro, *Int. Dairy J.*, 2007, **17**, 1188–1194.
22 F. Shapiro and N. Silanikove, *Food Chem.*, 2010, **119**, 829–833.
23 K. A. Gumaa, F. Novello and P. McLean, *Biochem. J.*, 1969, **114**, 253–264.
24 D. A. Rokosh, W. G. W. Kurtz and T. A. Laure, *Anal. Biochem.*, 1973, **54**, 477–483.
25 T. Larsen, *J. Dairy Res.*, 2005, **72**, 209–216.
26 E. Feldman, http://www.amdcc.org/shared/showFile.aspx?doctypeid=3&docid=33, 2004, Version 1, 1–3.
27 SAS Institute, *SAS version 9.2*, SAS Institute, Cary, NC, U.S.A., 2009.
28 Y. Lavon, G. Leitner, T. Goshen, R. Braw-Tal, S. Jacoby and D. Wolfenson, *Theriogenology*, 2008, **70**, 956–967.
29 N. Silanikove, U. Merin and G. Leitner, *RSC Adv.*, 2014b, **4**, 26476–26486.
30 M. Klein, M. Almstetter, N. Nuernberger, G. Sigl, W. Gronwald, S. Wiedemann, K. Dettmer and P. Oefner, *J. Proteome Res.*, 2013, **12**, 5223–5232.
31 M. R. Grigor and P. E. Hartmann, *J. Dairy Res.*, 1985, **52**, 501–506.
32 S. Purup and T. S. Nielsen, *Animal*, 2012, **6**, 423–432.
33 A. Shamay, E. Zeelon, Z. Ghez, N. Cohen, A. G. Mackinlay and A. Gertler, *J. Endocrinol.*, 1987, **113**, 81–88.
34 K. K. Piotrowska-Tomala, M. M. Bah, K. Jankowska, K. Lukasik, P. Warmowski, A. M. Galvao and D. J. Skarzynski, *Domest. Anim. Endocrinol.*, 2015, **52**, 90–99.
35 K. Kobayashi, C. Kuki, S. Oyama and H. Umura, *Exp. Cell Res.*, 2016, **340**, 295–304.
36 K. K. Piotrowska-Tomala, M. J. Siemieniuch, A. Z. Szóstek, A. J. Korzekwa, I. Woclawek-Potocka, A. M. Galváo, K. Okuda and D. J. Skarzynski, *Domest. Anim. Endocrinol.*, 2012, **43**, 278–288.
37 J. Denis-Robichaud, J. Dubuc, D. Lefebvre and L. DesCoteaux, *J. Dairy Sci.*, 2014, **97**, 3364–3370.
38 G. Leitner, U. Merin and N. Silanikove, *Int. Dairy J.*, 2011, **21**, 279–285.
39 N. Silanikove, U. Merin and G. Leitner, *Int. Dairy J.*, 2006, **16**, 535–545.
40 N. Silanikove, U. Merin and G. Leitner, *Small Rumin. Res.*, 2014c, **122**, 76–82.
41 D. B. Shennan and M. Peaker, *Physiol. Rev.*, 2000, **80**, 925–951.
42 M. Li, X. Liu, G. Robinson, U. Bar-Peled, K. U. Wagner, W. S. Young, L. Hennighausen and P. A. Furth, *Proc. Natl. Acad. Sci. U. S. A.*, 1997, **94**, 3425–3430.
43 R. M. Loftus and D. K. Finlay, *J. Biol. Chem.*, 2016, **291**, 1–10.
44 L. D. Plank, A. B. Connolly and G. L. Hill, *Ann. Surg.*, 1998, **228**, 146–158.
45 M. R. Waldron, A. E. Kulick, A. W. Bell and T. R. Overton, *J. Dairy Sci.*, 2006, **89**, 596–610.
46 A. Stincone, A. Prigione, T. Cramer, M. Wamelink, K. Campbell, E. Cheung, V. Olin-Sandoval, N. M. Grüning, A. Krüger, M. Tauqeer Alam and M. A. Keller, *Biol. Rev.*, 2015, **90**, 927–963.
47 K. C. Patra and N. Hay, *Trends Biochem. Sci.*, 2014, **39**, 347–354.
48 C. J. Schofield and P. J. Ratcliffe, *Nat. Rev. Mol. Cell Biol.*, 2004, **5**, 343–354.
49 L. Connelly, W. Barham, R. Pigg, L. Saint-Jean, T. Sherrill, D. S. Cheng, L. A. Chodosh, T. S. Blackwell and F. E. Yull, *J. Cell. Physiol.*, 2010, **222**, 73–81.
50 S. R. Davis and R. J. Collier, *J. Dairy Sci.*, 1985, **68**, 1041–1058.
51 E. Delamaire and J. Guinard-Flament, *J. Dairy Sci.*, 2006, **89**, 3439–3446.
52 L. R. Stein and I. S. Imai, *Trends Endocrinol. Metab.*, 2012, **23**, 420–428.
53 P. Belenky, K. L. Bogan and C. Brenner, *Trends Biochem. Sci.*, 2006, **32**, 12–19.
54 W. Ying, *Front. Biosci.*, 2005, **11**, 3129–3148.
55 P. H. Williamson, P. Lund and H. A. Krebs, *Biochem. J.*, 1967, **103**, 514–527.
56 F. Sun, C. Dai, J. Xie and X. Hu, *PLoS One*, 2012, **7**, e34525.
57 V. Nizet and R. S. Johnson, *Nat. Rev. Immunol.*, 2009, **9**, 609–617.
58 C. Peyssonnaux, P. Cejudo-Martin, A. Doedens, A. S. Zinkernagel, R. S. Johnson and V. Nizet, *J. Immunol.*, 2007, **178**, 7516–7519.

59 P. G. Haji-Michael, L. Ladrière, A. Sener, J. L. Vincent and W. J. Malaisse, *Metabolism*, 1999, **48**, 779–785.
60 J. Bakker, M. W. N. Nijsten and T. C. Jansen, *Ann. Intensive Care*, 2013, **3**, 1–8.
61 P. T. Chun, R. J. McPherson, L. C. Marney, S. Z. Zangeneh, B. A. Parsons, A. Shojaie, R. E. Synovec and S. E. Juul, *Dev. Neurosci.*, 2015, **37**, 161–171.
62 L. G. Forni, W. McKinnon, G. A. Lord, D. F. Treacher, J. M. R. Peron and P. J. Hilton, *Crit. Care*, 2005, **9**, R591.
63 S. Pavlides, D. Whitaker-Menezes, R. Castello-Cros, N. Flomenberg, A. K. Witkiewicz, P. G. Frank, M. C. Casimiro, C. Wang, P. Fortina, S. Addya and R. G. Pestell, *Cell Cycle*, 2009, **8**, 3984–4001.
64 U. E. Martinez-Outschoorn, R. M. Balliet, D. Rivadeneira, B. Chiavarina, S. Pavlides, C. Wang, D. Whitaker-Menezes, K. Daumer, Z. Lin, A. Witkiewicz and N. Flomenberg, *Cell Cycle*, 2010, **9**, 3276–3296.
65 U. E. Martinez-Outschoorn, M. P. Lisanti and F. Sotgia, *Semin. Cancer Biol.*, 2014, **25**, 47–60.